Journal of Computational and Applied Mathematics 234 (2010) 3373–3386

Contents lists available at ScienceDirect

Journal of Computational and Applied Mathematics

journal homepage: www.elsevier.com/locate/cam

Error propagation in numerical approximations near relative equilibria

J. Álvarez [a], A. Durán [b,*]

[a] Departamento de Matemática Aplicada, E.T.S. de Ingenieros Industriales, Universidad de Valladolid, Paseo del Cauce s/n, E-47011 Valladolid, Spain

[b] Departamento de Matemática Aplicada, E.T.S.I. de Telecomunicación, Universidad de Valladolid, Campus Miguel Delibes, Camino del Cementerio s/n E-47011 Valladolid, Spain

ARTICLE INFO

Article history:
Received 9 April 2008
Received in revised form 10 March 2010

MSC:
65L99
65L05
65Z05
70H33
37J15

Keywords:
Conservative numerical methods
Error propagation
Relative equilibria
Symmetries of differential equations

ABSTRACT

We study the propagation of errors in the numerical integration of perturbations of relative equilibrium solutions of Hamiltonian differential equations with symmetries. First it is shown that taking an initial perturbation of a relative equilibrium, the corresponding solution is related, in a first approximation, to another relative equilibrium, with the parameters perturbed from the original. Then, this is used to prove that, for stable relative equilibria, error growth with respect to the perturbed solution is in general quadratic, but only linear for schemes that preserve the invariant quantities of the problem. In this sense, the conclusion is similar to the one obtained when integrating unperturbed relative equilibria. Numerical experiments illustrate the results.

1. Introduction

The purpose of this paper is to study the propagation of errors in the numerical integration of some perturbations of relative equilibrium solutions of canonical autonomous Hamiltonian systems

$$\dot{z} = J\nabla H(z), \quad z \in \Omega. \tag{1}$$

In (1) Ω is a domain of $\mathcal{R}^{2n}$, J is the skew-symmetric matrix

$$J = \begin{pmatrix} 0 & -I_n \\ I_n & 0 \end{pmatrix},$$

where I_n is the identity matrix of order n and $H : \Omega \to \mathcal{R}$ is the Hamiltonian.

In the analysis of the numerical integration of differential equations, there are some numerical properties, apart from the classical of consistency, stability and convergence, that have to be taken into account when choosing a method to integrate a differential equation. Sometimes these numerical properties arise from a purpose of emulating or preserving some physical or geometrical aspect of the differential system to be integrated, or because of special properties of the solutions to be simulated. Thus, it seems reasonable to think that those geometric numerical methods [1,2] that consider such properties in their design will give a more positive response, in some sense, than a general integrator. They have been applied and analyzed in different problems. Many of them concern ordinary differential equations, especially Hamiltonian and reversible

* Corresponding author.
E-mail addresses: joralv@eis.uva.es (J. Álvarez), angel@mac.uva.es (A. Durán).

0377-0427/$ – see front matter © 2010 Elsevier B.V. All rights reserved.
doi:10.1016/j.cam.2010.04.038

systems (see e.g. [3,1,4,5] and references therein, for some review of the methods; the papers [6–16] may be cited as a modest representation of more specific works). Some other studies have treated some cases of partial differential equations, like [17,5,18–26] for instance.

This paper is in the context of long time integration of relative equilibria. Explicitly, our numerical problem is the time propagation of the error when approximating perturbations of relative equilibria and the property to be considered in the numerical integration is the conservation of quantities associated to the differential equations under study.

The presence, in Hamiltonian systems like (1), of first integrals different from the Hamiltonian H, is important in several aspects. From a geometrical and physical point of view, they generate symmetry groups of the system [27]. These are transformations that take solutions into other solutions. In the context of the integrability of the problem, the invariant quantities may be used to obtain a reduced Hamiltonian system with fewer variables. Each solution of the original system can be obtained from one of the reduced system by quadrature. This reduction is formed basically in two steps [28,29,27]: first, one restricts the original system to a fixed level set of the invariants and then the points in a same orbit of the symmetry group are identified as a point of the reduced phase space.

Although the number of invariants is not sufficient to integrate completely the problem, a special kind of solutions may be obtained, the so called relative equilibrium solutions [30]. In Hamiltonian systems like (1), a relative equilibrium is an equilibrium of the Hamiltonian subject to specific level sets of the invariants. In the context of the reduction previously described, relative equilibria correspond to equilibria of the reduced system. The solutions of the original system obtained from relative equilibria as initial data are determined by the symmetry group in a direct, simple way. The process makes these solutions depend on two types of parameters: first, there are parameters associated to the symmetry group; on the other hand, some other parameters determine the level set of the invariants at the original relative equilibria. These last parameters are related to the Lagrange multipliers of the restricted Hamiltonian problem of which the relative equilibria are solutions.

The interest of relative equilibria is shown in some applications. We just comment on three of them. For example (see [28] and references therein), in ordinary differential equations, they may appear as special orbits of mechanical systems, such as rigid body systems, and it may be interesting to study their stability, in order to for instance, design artificial satellites remaining in them. Another example concerns partial differential equations. In classical Hamiltonian nonlinear wave equations, relative equilibria may correspond to an important kind of waves, which are the solitary waves (see e.g. [31] an references therein). The study of several types of stability of these waves, or interactions between themselves and with other waves may be approached within the framework of the relative equilibria theory. A final point concerns the study of relative periodic orbits [28,29]. They are periodic solutions of the reduced system and sometimes appear as perturbations of relative equilibria (see [32] and references therein).

As far as the numerical integration of relative equilibrium solutions is concerned, the references [33,34] are relevant. The numerical problem they focus on consists of raising if the conservation of invariant quantities of the problem shows some influence in the efficiency of a numerical method when simulating this kind of solutions. More explicitly, in [34], the propagation of errors in the numerical integration of relative equilibria is studied. The main conclusion there states that the error propagation when integrating stable relative equilibria of Hamiltonian problems behaves better for numerical methods that conserve invariant quantities of the problem. For this kind of methods, error grows linearly in time, while for general schemes, the growth is quadratic. The numerical solution approximates to a new 'relative equilibrium'; this differs from the original one in terms that depend on the conservative character of the scheme. A general numerical solution separates from the original relative equilibrium solution by modifying its two types of parameters. The perturbation in the group parameters is quadratic in time, while the modification in the level set parameters grows linearly with time. In the case of a numerical solution given by a conservative scheme, these last parameters remain unaltered; the modified relative equilibrium, which is better approximated by the numerical solution than the exact one, remains in the original level set of the invariants. Only a linear growth in the perturbation of the symmetry group parameters is observed. Finally, a cheap modification of a conservative scheme allows to annihilate this growth and thus obtains a bounded behaviour of the errors [33].

In this paper we analyze a similar numerical problem for the case of integrations of solutions obtained from an initial perturbation of a relative equilibrium. The results are orientated in two directions. First, we establish that the solution coming from an initial perturbation of a relative equilibrium can be typically written, in a first approximation, as a sum of two terms. The first one is a relative equilibrium with parameters perturbed from the original. The second term may remain bounded in time and, depending on the direction of the initial perturbation, may not appear. Secondly, as far as the time propagation of the errors is concerned, we obtain a similar conclusion to that of [34]. The advantages of the conservative methods in the numerical integration of relative equilibria are extended to the case of the integration of this type of perturbations of relative equilibria, at least for moderate times. While for a general method errors grow quadratically in time, a method that preserves invariants of the problem provides an error that only grows linearly with time.

The paper is structured as follows. Section 2 summarizes some basic results about Hamiltonian relative equilibrium problems. For simplicity we only consider one-parameter symmetry groups, but the extension to Abelian, multi-parameter symmetry groups may be done with not much more effort. This section also incorporates the analysis about the structure of solutions obtained from a perturbation of a relative equilibrium. This includes the study of the homogeneous variational equation that arises from the linearization around a relative equilibrium. This study will be used in Section 3, which is devoted to the problem of the numerical approximation. The analysis of the global error in the numerical integration of the perturbed problem allows to obtain the asymptotic behaviour of the numerical approximation. This includes the

unperturbed case, treated in [34]. With this expansion, we can identify the mechanisms that lead to a favourable error propagation with respect to the perturbed solution in conservative methods. Finally, Section 4 contains the numerical illustration of the previous results. It is divided into two parts. In the first one, the structure of the perturbed solution obtained in Section 2 is illustrated. Here we use a high order method to integrate a test problem with different types of perturbations. In the second part, we illustrate the different asymptotic behaviour of the numerical approximations, from the expansion obtained in Section 3. Here we analyze the error generated by two methods, that have been selected as examples of conservative and nonconservative schemes.

2. Hamiltonian relative equilibria and perturbations

2.1. Preliminaries

The mathematical framework of this paper is similar to that of [33]. We assume that (1) has a first integral $I : \Omega \to \mathcal{R}$, different from the Hamiltonian H and which is not a distinguished function [27]. This implies that the Hamiltonian vector field $g = J\nabla I$ is the infinitesimal generator of a one-parameter symmetry group of (1)

$$\mathbf{G} = \{G_s = \varphi_{s,g} : s \in \mathcal{R}\}.$$

Here, $\varphi_{s,g}$ denotes the flow associated to g and it is supposed that, for each s, the domain of the diffeomorphism $\varphi_{s,g}$ is the whole Ω, as well as the flow φ_t of the system (1). The symmetry group condition means that the flow φ_t commutes with the elements G_s, $s \in \mathcal{R}$ of the group.

We assume that (1) admits special solutions of the form

$$z(t) = G_{\lambda_0 t}(z_0), \tag{2}$$

for $\lambda_0 \in \mathcal{R}$, $z_0 \in \Omega$. In order to (2) be a solution of (1), the initial state z_0 must be a relative equilibrium [30,28]. This means that z_0 is an equilibrium of the Hamiltonian restricted to a level set of the invariant I,

$$\nabla\,(H(z_0) - \lambda_0 I(z_0)) = 0, \tag{3}$$

$$I(z_0) = c_0. \tag{4}$$

It can be seen that any element $G_s(z_0)$ of the orbit of the symmetry group $\mathbf{G}$ through z_0 satisfy (3) and (4). Therefore, the relative equilibrium z_0 depends on two parameters: the first one is the parameter s_0 of the symmetry group; the second one is a level set parameter c_0 or, alternatively, the multiplier λ_0. We will denote $z_0 = z(s_0, \lambda_0)$.

The presence of the first integral I, and therefore of the Hamiltonian symmetry group G, allows to study (1) by means of a reduced Hamiltonian system with two fewer variables. For a description, in local coordinates, of the reduction for this kind of symmetry groups, see [34]. A more general explanation of the reduction process by using more general symmetry groups can be seen e.g. in [30,27]. The reduced system is obtained in two stages, which correspond to constraining the original system to a level set of I and to identifying points in the same orbit of $\mathbf{G}$. This reduced system controls the evolution of the orbits of the group. The properties of the reduction which are now relevant for us are two. First, it is known that the group orbit through relative equilibria are equilibria of the reduced system [30]. Relative equilibria give rise, in the original system, to solutions (2), determined, in a certain way, by the symmetry group and the corresponding level set (4). They project to an equilibrium of the reduced system. On the other hand, it is also known (see [33,34] and references therein) that, if the orbit of the relative equilibrium $z_0 = z(s_0, \lambda_0)$ is nondegenerate as an equilibrium of the reduced system, then near z_0 every relative equilibrium is of the form $z(s, c) = G_s(z(c))$ with $z(c)$ a solution of

$$\nabla\,(H(z(c)) - \lambda(c) I(z(c))) = 0,$$

$$I(z(c)) = c,$$

for c close to c_0 and a multiplier $\lambda = \lambda(c)$. For convenience, in what follows we assume that

$$\left.\frac{\partial \lambda(c)}{\partial c}\right|_{c=c_0} \neq 0,$$

and we denote $z(s, c)$ by $z(s, \lambda)$. A recent theory for relative equilibria in the case $\frac{\partial \lambda(c)}{\partial c}|_{c=c_0} = 0$ can be seen in [35].

Although the previous description was, for simplicity, done for only one first integral, a generalization to Abelian, multi-parameter symmetry groups, involving more than one conserved quantity is admissible, see [34].

2.2. Structure of perturbations of relative equilibria

The main goal of this work is to study the time behaviour of numerical integrators when approximating solutions coming from initial perturbations of relative equilibria. We first need to obtain some information about the perturbed solutions.

Our first results state a certain structure in these solutions. Let $z_0 = z(s_0, \lambda_0)$ be a relative equilibrium whose orbit by the group **G** is nondegenerate as equilibrium of the reduced system. For ϵ small and $v_0 \in \mathcal{R}^{2n}$, the solution of (1) with initial condition $z_0 + \epsilon v_0$ can be formally written in the form

$$z(t) + \epsilon v(t) + O(\epsilon^2), \tag{5}$$

where $z(t)$ is given by (2) and $v(t)$ is the solution of the initial value problem for the variational equation

$$\begin{aligned} \dot{v}(t) &= JH''(z(t))v(t) \\ v(0) &= v_0. \end{aligned} \tag{6}$$

In (6) H'' denotes the Hessian of H. The symmetry group **G** determines the form of the solution of (6). It is well known [34] that $v(t)$ can be expressed as

$$v(t) = G'_{t\lambda_0}(z(s_0, \lambda_0))V(t),$$

where $V(t)$ is the solution of

$$\dot{V}(t) = LV(t) \tag{7}$$

$$V(0) = v_0, \tag{8}$$

for L the constant coefficient matrix

$$L = JS, \quad S = H''(z(s_0, \lambda_0)) - \lambda_0 I''(z(s_0, \lambda_0)).$$

As L is of constant coefficient type, the solution of (7) and (8) is of the form

$$V(t) = \mathrm{e}^{tL} v_0. \tag{9}$$

In order to describe (9) in more detail, we need some spectral information about L. This is basically given by Theorem 3.1 of [33,34]. Here we reproduce the most relevant results for the paper.

Theorem 1. *Suppose that $z(s_0, \lambda_0)$ is a solution of (3) and (4) whose orbit by **G** is nondegenerate as equilibrium of the reduced system and that $\frac{\partial \lambda(c)}{\partial c}|_{c=c_0} \neq 0$. Then*

(i) *Zero is an eigenvalue of L with geometric multiplicity one and algebraic multiplicity two. The set*

$$\left\{ J\nabla I(z(s_0, \lambda_0)), \left.\frac{\partial z(s_0, \lambda)}{\partial \lambda}\right|_{\lambda=\lambda_0} \right\}, \tag{10}$$

is a basis of the generalized kernel $\mathrm{Ker}_g L = \mathrm{Ker}\, L^2$ *with*

$$L \left.\frac{\partial z(s_0, \lambda)}{\partial \lambda}\right|_{\lambda=\lambda_0} = J\nabla I(z(s_0, \lambda_0)).$$

(ii) *Let M be the unique L-invariant supplementary subspace in $\mathcal{R}^{2n}$ of the generalized kernel of L. Denote by $\widehat{L}$ the restriction of L to M. Then, the eigenvalues and Jordan structure of $\widehat{L}$ coincide with those of the matrix of the linearization of the reduced system around the orbit of $z(s_0, \lambda_0)$.*

Coming back to (9), note first that we can decompose

$$v_0 = v_{\mathrm{Ker}} + v_M, \tag{11}$$

where $v_{\mathrm{Ker}} \in \mathrm{Ker}_g L$, $v_M \in M$. At the same time, we know that v_{Ker} is of the form

$$v_{\mathrm{Ker}} = \alpha_0 J\nabla I(z(s_0, \lambda_0)) + \beta_0 \left(\left.\frac{\partial z(s_0, \lambda)}{\partial \lambda}\right|_{\lambda=\lambda_0} \right),$$

for certain constants α_0, β_0. Then we can write the solution (9) as

$$V(t) = \alpha_0 J\nabla I(z(s_0, \lambda_0)) + \beta_0 \left(\left.\frac{\partial z(s_0, \lambda)}{\partial \lambda}\right|_{\lambda=\lambda_0} + tJ\nabla I(z(s_0, \lambda_0)) \right) + \mathrm{e}^{t\hat{L}} v_M. \tag{12}$$

The constants α_0, β_0 can be determined in terms of the basis of the generalized kernel of the adjoint of L, $L^* = -SJ$ [33]

$$\{\nabla I(z(s_0, \lambda_0)), \Psi(z(s_0, \lambda_0))\}, \tag{13}$$

where $\Psi(z(s_0,\lambda_0)) = J\partial z(s_0,\lambda)/\partial\lambda|_{\lambda=\lambda_0}$. The bases (10) and (13) are biorthogonal and therefore

$$\alpha_0 = \frac{\Psi(z(s_0,\lambda_0))^T v_0}{(J\nabla I(z(s_0,\lambda_0)))^T \Psi(z(s_0,\lambda_0))} = \frac{\Psi(z(s_0,\lambda_0))^T v_0}{\frac{\mathrm{d}}{\mathrm{d}\lambda} I(z(s_0,\lambda))\big|_{\lambda=\lambda_0}}, \tag{14}$$

$$\beta_0 = \frac{\nabla I(z(s_0,\lambda_0))^T v_0}{\nabla I(z(s_0,\lambda_0))^T \frac{\partial z(s_0,\lambda)}{\partial\lambda}\Big|_{\lambda=\lambda_0}} = \frac{\nabla I(z(s_0,\lambda_0))^T v_0}{\frac{\mathrm{d}}{\mathrm{d}\lambda} I(z(s_0,\lambda))\big|_{\lambda=\lambda_0}}. \tag{15}$$

The structure of solutions of (6) allows to obtain a result about the form of solutions of system (1) generated from an initial perturbation of a relative equilibrium. At the ϵ order, they consist of a perturbed relative equilibrium plus complementary terms.

Theorem 2. *Assume that* $\frac{\partial\lambda(c)}{\partial c}|_{c=c_0} \neq 0$ *and that* $z(s_0,\lambda_0)$ *is nondegenerate as equilibrium of the reduced system. Then, for* ϵ *small and* $v_0 \in \mathcal{R}^{2n}$, *the solution* $z(t,\epsilon)$ *of the initial value problem given by* (1) *with* $z(0) = z(s_0,\lambda_0) + \epsilon v_0$ *can be written as*

$$z(t,\epsilon) = G_{(\lambda_0+\epsilon\beta_0)t}(z(s_0+\epsilon\alpha_0, \lambda_0+\epsilon\beta_0)) + \epsilon\rho(t) + O(\epsilon^2), \tag{16}$$

where

(i) α_0, β_0 *are constants given by* (14) *and* (15).
(ii) *The function* $\rho(t)$ *is independent of* ϵ. *If the symmetry group* **G** *consists of isometries and the relative equilibrium is stable (as equilibrium of the reduced system), then* $\rho(t)$ *is bounded for* $t \geq 0$.

Proof. As we have seen in (12), the solution of the perturbed problem is of the form (5) with

$$\begin{aligned} z(t) &= G_{t\lambda_0}(z(s_0,\lambda_0)),\\ v(t) &= G'_{t\lambda_0}(z(s_0,\lambda_0))V(t)\\ &= G'_{t\lambda_0}(z(s_0,\lambda_0))\left[\alpha_0 J\nabla I(z(s_0,\lambda_0)) + \beta_0\left(\frac{\partial z(s_0,\lambda)}{\partial\lambda}\Big|_{\lambda=\lambda_0} + tJ\nabla I(z(s_0,\lambda_0))\right) + \mathrm{e}^{t\hat{L}}v_M\right], \end{aligned}$$

where the decomposition of v_0 expressed in (11) is used, α_0, β_0 are given by (14) and (15) and $v_M \in M$. Then

$$\begin{aligned} z(t,\epsilon) &= G_{t\lambda_0}(z(s_0,\lambda_0)) + \epsilon G'_{t\lambda_0}(z(s_0,\lambda_0))\left[\alpha_0 J\nabla I(z(s_0,\lambda_0)) + \beta_0\left(\frac{\partial z(s_0,\lambda)}{\partial\lambda}\Big|_{\lambda=\lambda_0} + tJ\nabla I(z(s_0,\lambda_0))\right)\right]\\ &\quad + \epsilon G'_{t\lambda_0}(z(s_0,\lambda_0))\mathrm{e}^{t\hat{L}}v_M + O(\epsilon^2). \end{aligned} \tag{17}$$

We define $\rho(t) = G'_{t\lambda_0}(z(s_0,\lambda_0))\mathrm{e}^{t\hat{L}}v_M$. On the other hand, since [34]

$$J\nabla I(G_{t\lambda_0}(z(s_0,\lambda_0))) = G'_{t\lambda_0}(z(s_0,\lambda_0))J\nabla I(z(s_0,\lambda_0)),$$

then, if we expand the first term on the right hand side of (16) in powers of ϵ, we have

$$\begin{aligned} G_{(\lambda_0+\epsilon\beta_0)t}(z(s_0+\epsilon\alpha_0,\lambda_0+\epsilon\beta_0)) &= G_{t\lambda_0}(z(s_0,\lambda_0)) + t\epsilon\beta_0\frac{\mathrm{d}}{\mathrm{d}\tau}G_\tau(z(s_0,\lambda_0))\Big|_{\tau=t\lambda_0}\\ &\quad + G'_{t\lambda_0}(z(s_0,\lambda_0))\left(\epsilon\alpha_0\frac{\partial z(s,\lambda_0)}{\partial s}\Big|_{s=s_0} + \epsilon\beta_0\frac{\partial z(s_0,\lambda)}{\partial\lambda}\Big|_{\lambda=\lambda_0}\right) + O(\epsilon^2)\\ &= G_{t\lambda_0}(z(s_0,\lambda_0)) + t\epsilon\beta_0 J\nabla I(G_{t\lambda_0}(z(s_0,\lambda_0)))\\ &\quad + G'_{t\lambda_0}(z(s_0,\lambda_0))\left(\epsilon\alpha_0 J\nabla I(z(s_0,\lambda_0)) + \epsilon\beta_0\frac{\partial z(s_0,\lambda)}{\partial\lambda}\Big|_{\lambda=\lambda_0}\right) + O(\epsilon^2)\\ &= G_{t\lambda_0}(z(s_0,\lambda_0)) + \epsilon G'_{t\lambda_0}(z(s_0,\lambda_0))\Bigg(\alpha_0 J\nabla I(z(s_0,\lambda_0))\\ &\quad + \beta_0\left(\frac{\partial z(s_0,\lambda)}{\partial\lambda}\Big|_{\lambda=\lambda_0} + tJ\nabla I(z(s_0,\lambda_0))\right)\Bigg) + O(\epsilon^2), \end{aligned}$$

which differs from the first three terms on the right hand side of (17) in $O(\epsilon^2)$ terms. Finally, from the definition of the function $\rho(t)$, we have that if the symmetry group consists of isometries, then $\|G'_{t\lambda_0}(z(s_0,\lambda_0))\| = 1$ for $t \geq 0$. If, furthermore, the relative equilibrium is stable, since $\rho(t)$ is a solution of the homogeneous variational equation in the supplementary subspace M, then (ii) of Theorem 1 shows that it is bounded for $t \geq 0$. □

Note that the form (16) could be considered as a first approximation to the idea of a more general structure of the perturbed solution. This has been applied to some studies of the stability of solitary waves (see e.g. [36]). The strategy assumes a more general ansatz about the form of the perturbed solution, as a sum of a relative equilibrium profile, but with time dependent parameters, plus another complementary term. This ansatz would allow to distinguish, at least in theory, the evolution of the parameters, through the modulation equations. The hypothesis is suggested by the numerical experiments about small perturbations of solitary waves of some nonlinear dispersive equations. Such experiments showed that the resulting solutions were decomposed into a dominant wave, tending to a solitary wave profile, plus a term involving dispersion and maybe some other smaller solitary waves.

In Section 4 we propose some numerical experiments with different types of perturbations. They illustrate the degree of approximation of this perturbed relative equilibrium to the solution $z(t,\epsilon)$ coming from the initial perturbation.

3. Numerical approximation

3.1. Introduction

In the previous section we have discussed the behaviour, in a first approximation, of the solutions of (1) obtained from an initial perturbation of a relative equilibrium. In this section we will study the time propagation of the errors in the numerical integration of these perturbed solutions.

We consider a one-step method of order $r \geq 1$ for (1)

$$Z_{n+1} = \psi_h(Z_n), \quad n = 0, 1, \ldots, \tag{18}$$

for a mapping $\psi_h : \Omega \to \Omega$, with h the stepsize. The hypotheses (A1) and (A2) in [34] about the numerical method are also assumed here for (18). Essentially, it is supposed the existence of asymptotic expansions of the local and global error, along with the assumption that the mapping ψ_h is invariant by the symmetry group **G**. These conditions are satisfied by all the methods used in practice.

Now, if (18) approximates the solution of (1), $z(t,\epsilon)$, where $z(0,\epsilon) = Z_0 = z(s_0,\lambda_0) + \epsilon v_0$, with $z(s_0,\lambda_0)$ a relative equilibrium, $v_0 \in \mathcal{R}^{2n}$ and ϵ small, then the global error $Z_n(\epsilon) - z(t_n,\epsilon)$ of (18) has an asymptotic expansion [37]

$$Z_n(\epsilon) - z(t_n,\epsilon) = h^r e(t_n,\epsilon) + h^r Q(t_n,h,\epsilon), \tag{19}$$

where e is a smooth function that satisfies the variational problem [37,38]:

$$\begin{aligned} &\dot{e}(t,\epsilon) = JH''(z(t,\epsilon))\cdot e(t,\epsilon) - l_{r+1}(z(t,\epsilon)), \\ &e(0,\epsilon) = 0, \end{aligned} \tag{20}$$

and Q is a remainder that, for fixed t and ϵ, tends to zero as $h \to 0$. In (20), l_{r+1} is the leading term of the asymptotic expansion of the local error. Some more terms in the expansion of the error might be included. The corresponding error functions would satisfy similar results to those of the leading term, explained below. For simplicity, we have preferred not to include them, see e.g. [39].

3.2. Behaviour in time of global error

If we expand the leading term of the global error in powers of ϵ

$$e(t,\epsilon) = e(t) + \epsilon e_1(t) + O(\epsilon^2), \tag{21}$$

and also the elements of (20), we have, by equating the coefficients of the powers of ϵ, the equations

$$\begin{aligned} &\dot{e}(t) = JH''(z(t))\cdot e(t) - l_{r+1}(z(t)), \\ &e(0) = 0, \end{aligned} \tag{22}$$

for the first term of (21) and

$$\begin{aligned} &\dot{e}_1(t) = JH''(z(t))\cdot e_1(t) + JH'''(z(t))v(t)e(t) - l'_{r+1}(z(t))v(t), \\ &e_1(0) = 0, \end{aligned}$$

for the second term, where $z(t) = G_{t\lambda_0}(z(s_0,\lambda_0))$ and $v(t)$ is the solution of (6). In order to analyze the time behaviour of the numerical methods when integrating perturbations of relative equilibria, we need some results about the two terms e and e_1 of (21). To this goal, we use the spectral properties of the linearization explained in Section 2.2.

As far as the unperturbed term $e(t)$ is concerned, the structure is already known, see [33]. We recall the corresponding result.

Theorem 3. *Suppose that* $\frac{\partial\lambda(c)}{\partial c}|_{c=c_0} \neq 0$ *and that* $z(s_0, \lambda_0)$ *in* (3) *and* (4) *is nondegenerate as equilibrium of the reduced system. Then the solution of* (22) *can be written in the form* $e(t) = G'_{\lambda_0 t}(z(s_0, \lambda_0))E(t)$ *with*

$$\begin{aligned} E(t) &= \int_0^t \mathrm{e}^{(t-\tau)L}\mathrm{d}\tau(-l_{r+1}(z(s_0, \lambda_0))) \\ &= t\alpha J\nabla I(z(s_0, \lambda_0)) + \beta\left(t\frac{\partial z(s_0, \lambda)}{\partial\lambda}\bigg|_{\lambda=\lambda_0} + \frac{t^2}{2}J\nabla I(z(s_0, \lambda_0))\right) + (\mathrm{e}^{t\hat{L}} - I)\hat{L}^{-1}l_M, \end{aligned}$$

where

(i) l_M *is the component of* $-l_{r+1}(z(s_0, \lambda_0))$ *in the supplementary subspace* M *of* $\mathrm{Ker}_g L$.
(ii) $\hat{L} = L|_M$.
(iii) α, β *are constants given by*

$$\alpha = -\frac{\Psi(z(s_0, \lambda_0))^T l_{r+1}(z(s_0, \lambda_0))}{(J\nabla I(z(s_0, \lambda_0)))^T\Psi(z(s_0, \lambda_0))} \tag{23}$$

$$\beta = -\frac{\nabla I(z(s_0, \lambda_0))^T l_{r+1}(z(s_0, \lambda_0))}{\nabla I(z(s_0, \lambda_0))^T\left.\frac{\partial z(s_0,\lambda)}{\partial\lambda}\right|_{\lambda=\lambda_0}}. \tag{24}$$

If $z(s_0, \lambda_0)$ *is stable as an equilibrium of the Hamiltonian reduced system, then the third term remains bounded for* $t \geq 0$.

As far as the term $e_1(t)$ is concerned, the most important thing is that its position in the asymptotic expansion of the global error gives rise to a term that for fixed t is $O(h^r\epsilon)$. Since $h^r\epsilon \leq h^{2r}/2 + \epsilon^2/2$, this term can be included in the remainders $O(h^{r+1})$ and $O(\epsilon^2)$.

3.3. Asymptotic behaviour of numerical integrators

The previous analysis of the leading term of the global error is the key to obtaining the following result. This explains, in a first approximation, the behaviour in time of numerical methods when integrating solutions of (1) from initial perturbations of relative equilibria.

Theorem 4. *Under the hypotheses of Section* 3.1, *suppose that* $\frac{\partial\lambda(c)}{\partial c}|_{c=c_0} \neq 0$ *and let* $z(s_0, \lambda_0)$ *be a relative equilibrium solution of* (3) *and* (4) *whose orbit by* **G** *is a nondegenerate equilibrium of the reduced system. Then, if* $Z_0 = z(s_0, \lambda_0) + \epsilon v_0$, $v_0 \in \mathcal{R}^{2n}$, *we have*

$$Z_n(\epsilon) = G_{t_n\bar{\lambda}}(z(\bar{s}, \bar{\bar{\lambda}})) + \epsilon\rho(t) + h^r G'_{t_n\lambda_0}(z(s_0, \lambda_0))(\mathrm{e}^{t_n\widehat{L}} - I)\widehat{L}^{-1}l_M + h^r q(h, t_n) + h^r\epsilon e_1(t) + O(\epsilon^2), \tag{25}$$

where

(i)

$$\begin{aligned} \bar{\lambda} &= \lambda_0 + \epsilon\beta_0 + \frac{t_n}{2}h^r\beta, \\ \bar{s} &= s_0 + \epsilon\alpha_0 + t_n h^r\alpha, \\ \bar{\bar{\lambda}} &= \lambda_0 + \epsilon\beta_0 + t_n h^r\beta, \end{aligned}$$

with the constants α_0, β_0 *given by* (14) *and* (15) *and the constants* α, β *given by* (23) *and* (24).
(ii) *The function* ρ *is given in Theorem* 2.
(iii) l_M *is the component of* $-l_{r+1}(z(s_0, \lambda_0))$ *in the supplementary subspace* M *of the generalized kernel of* L *and* $\hat{L} = L|_M$.
(iv) *The function* q *is a remainder that, for fixed* t, *tends to zero as* $h \to 0$.

Proof. Note first that, following Theorem 2, the solution of (1) with $z(0) = z(s_0, \lambda_0) + \epsilon v_0$ can be written in the form (16), with α_0, β_0 given by (14), (15). On the other hand, the leading term of the global error, by using Theorem 3, is of the form

$$\begin{aligned} e(t, \epsilon) &= e(t) + \epsilon e_1(t) + O(\epsilon^2) \\ &= G'_{t\lambda_0}(z(s_0, \lambda_0))\left(t\alpha J\nabla I(z(s_0, \lambda_0)) + \beta\left(t\frac{\partial z(s_0, \lambda)}{\partial\lambda}\bigg|_{\lambda=\lambda_0} + \frac{t^2}{2}J\nabla I(z(s_0, \lambda_0))\right)\right) \\ &\quad + G'_{t\lambda_0}(z(s_0, \lambda_0))\left((\mathrm{e}^{t\hat{L}} - I)\hat{L}^{-1}l_M\right) + \epsilon e_1(t) + O(\epsilon^2), \end{aligned} \tag{26}$$

with α, β given by (23), (24). Substituting (16) and (26) into (19) we have

$$\begin{aligned} Z_n(\epsilon) = {} & G_{(\lambda_0+\epsilon\beta_0)t_n}(z(s_0+\epsilon\alpha_0, \lambda_0+\epsilon\beta_0)) + h^r G'_{t_n\lambda_0}(z(s_0,\lambda_0))\left(t_n\alpha J\nabla I(z(s_0,\lambda_0))\right. \\ & \left. + \beta\left(t_n\frac{\partial z(s_0,\lambda)}{\partial\lambda}\bigg|_{\lambda=\lambda_0} + \frac{t_n^2}{2}J\nabla I(z(s_0,\lambda_0))\right)\right) + h^r G'_{t_n\lambda_0}(z(s_0,\lambda_0))\left((e^{t_n\hat{L}}-I)\hat{L}^{-1}l_M\right) \\ & + \epsilon h^r e_1(t_n) + \epsilon\rho(t_n) + h^r Q(t_n, h, \epsilon) + O(\epsilon^2). \end{aligned} \tag{27}$$

Finally, note that, by using an expansion in powers of h, the first four terms of (27) differ from the first term on the right hand side of (25) in $O(h^{2r})$ terms, that can be included in the remainder, along with the function Q. □

We make some comments about Theorem 4.

(1) The expansion (25) includes the unperturbed case, studied in [34]. For $\epsilon = 0$, the numerical solution is asymptotically a better approximation of a modified trajectory of $z(s_0, \lambda_0)$, trajectory with an error with respect to the original parameter λ_0 that in general grows linearly, and an error in the group parameters (phase error) $s_0 + \lambda_0 t$ that grows quadratically. In the case of a conservative scheme, we have $\beta = 0$ [34,22] and therefore the leading error in the parameter λ_0 does not grow with time and the phase error only grows linearly. Notice also that when the symmetry group consists of isometries and the relative equilibrium is stable, this is the dominant growth of the error, since in that case the complementary term is bounded in time.

(2) In the case of a perturbed solution, some components appear in the asymptotic expansion of the numerical approximation. First of all, the original trajectory is modified both by the initial perturbation of the relative equilibrium, in the sense of Theorem 2, and by the numerical method, in the same sense as in the unperturbed case. The first term is a 'modified perturbed relative equilibrium'; it is the perturbed relative equilibrium but with the parameters modified by the numerical method through the constants α and β. Note that if the reference is the perturbed relative equilibrium that appears in Theorem 2, the error with respect to the perturbed parameter $\lambda_0 + \epsilon\beta_0$ is in general linear in time, while the error with respect to the perturbed group parameters grows quadratically. Again, the fact that the method is conservative, acts in favour of the propagation. In this case, the numerical approximation does not commit the first approximation error in the parameter $\lambda_0 + \epsilon\beta_0$, while the error with respect to the perturbed group parameters only grows linearly with time. Therefore, the advantages in the use of conservative schemes obtained in [34] for time simulations of relative equilibria also appear in the case of solutions coming from initial perturbations of relative equilibria, at least in a first approximation and for moderate values of time. The expansion continues with two complementary terms, $\epsilon\rho(t)$, which is provided by the perturbation, and $G'_{t_n\lambda_0}(z(s_0,\lambda_0))\left((e^{t_n\hat{L}}-I)\hat{L}^{-1}l_M\right)$, provided by the numerical integrator. Both are bounded in time if the relative equilibrium is stable and the symmetry group consists of isometries. The expansion is completed by the remainders $O(\epsilon^2)$, $O(h^{r+1})$ and the term $h^r\epsilon e_1(t)$, that can be included in them.

As it can be inferred from the proof of Theorem 4, the growth of the remainder $h^r q + \epsilon h^r e_1$ in (25) is not uniform. This may limit the time for which the numerical solution is controlled by the first three terms of (25). In the numerical experiments below, the dominance of these terms is observed for moderate values of time.

4. Numerical experiments

4.1. Introduction

In this section we will show some numerical experiments in order to illustrate the previous results.
Our test problem will be the two-body problem explained in [33]. The Hamiltonian is $H = T + V$,

$$T = \frac{1}{2}(p_1^2 + p_2^2 + p_3^2 + p_4^2),$$
$$V = -\frac{1}{\sqrt{q_1^2+q_2^2}} - \frac{1}{\sqrt{q_3^2+q_4^2}} - \frac{\delta}{\sqrt{(q_1-q_3)^2+(q_2-q_4)^2}},$$

where δ is a positive parameter. The quantity

$$I = p_2q_1 - p_1q_2 + p_4q_3 - p_3q_4$$

is a first integral and generates a symmetry group consisting of rotations. Relative equilibrium solutions for the problem are of the form [33]

$$\begin{aligned} z(t,\lambda,s_0) &= G_{\lambda t+s_0}((0,\lambda r,0,-\lambda r,r,0,-r,0)) \\ &= (-\lambda r\sin(\lambda t+s_0), \lambda r\cos(\lambda t+s_0), \lambda r\sin(\lambda t+s_0), \\ &\quad -\lambda r\cos(\lambda t+s_0), r\cos(\lambda t+s_0), r\sin(\lambda t+s_0), -r\cos(\lambda t+s_0), -r\sin(\lambda t+s_0)) \end{aligned} \tag{28}$$

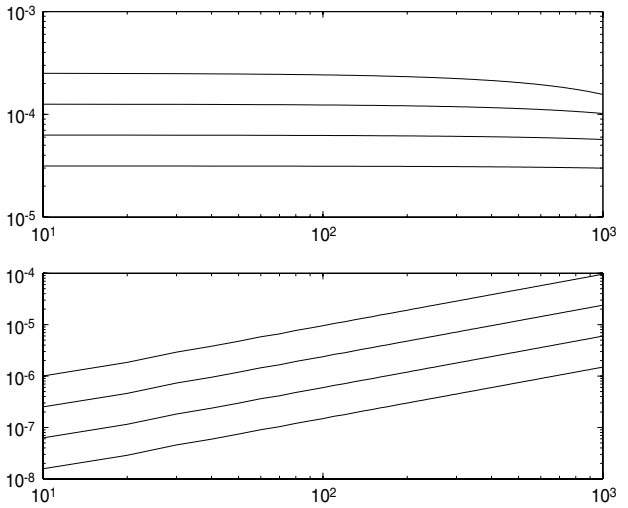

Fig. 1. Numerical illustration of (16), with $v_0 = J\nabla I(z(s_0, \lambda_0))$ and $\epsilon = 1.25\text{E}{-}04, 6.25\text{E}{-}05, 3.125\text{E}{-}05, 1.5625\text{E}{-}05$. Top: ERROR1 against time. Bottom: ERROR2 against time. The scale is logarithmic.

with r given by

$$r^3 = \frac{1}{\lambda^2}\left(1 + \frac{\delta}{4}\right).$$

This section will have two objectives: first, we will illustrate formula (16) by using different perturbations and a high order scheme to integrate the problem. In a second group of experiments, we will show the different behaviour of conservative and nonconservative methods in the long time integration of solutions coming from initial perturbations of relative equilibria. This will illustrate formula (25) in its different terms.

For both kinds of experiments we have considered a relative equilibrium $z(s_0, \lambda_0)$ given by (28) at $t = 0$ with $s_0 = 0, r = 1, \lambda_0 = \sqrt{1+\delta/4}, \delta = 0.1$, which is linearly stable [34]. From this relative equilibrium, we have used perturbations of two types: perturbations in the direction of $\text{Ker}_g L$ and general perturbations, with components in both directions.

4.2. Numerical illustration of the structure of perturbed solutions

The experiments performed in this subsection want to illustrate different aspects of formula (16). We have started from a perturbation of the relative equilibrium

$$z(s_0, \lambda_0) + \epsilon v_0,$$

with different values of ϵ and v_0. Then we have computed a numerical integration up to a moderate final time. The computation has been performed by using a high order method, to have a sufficiently good approximation. For our purposes we have used the four-stage Gauss method [37], with order $r = 8$. The method preserves the invariant I of the problem (in fact, Gauss methods preserve any quadratic invariant to machine accuracy [40]).

The general description of this first type of experiments is the following. For each considered perturbation, by using the four-stage Gauss method with $h = 1\text{E}{-}02$, we have integrated the initially perturbed problem up to $t = 1000$. The corresponding numerical solution will be considered as 'exact'. By using different values of ϵ, we have measured two errors: first, the difference (which will be denoted by ERROR1) between the numerical solution and the relative equilibrium solution without perturbation; secondly, the difference (ERROR2) between the numerical solution and the perturbed relative equilibrium, which is the first term on the right hand side of (16).

First perturbation

Here we have considered $v_0 = J\nabla I(z(s_0, \lambda_0))$. In this case, the perturbation has a unique component, in the direction of $\text{Ker}\, L$ [33]. This gives rise to $\alpha_0 = 1$, $\beta_0 = 0$, $v_M = 0$ in formula (16). The results are shown in Fig. 1.

We first observe that when these values of ϵ are considered, the error with respect to the perturbed relative equilibrium (Fig. 1, bottom) is smaller than the one with respect to the unperturbed relative equilibrium (Fig. 1, top). We also note that, when ϵ is divided by two, ERROR1 is also divided by two; this is a $O(\epsilon)$ difference, due to the term $\epsilon\alpha_0 J\nabla I(z(s_0, \lambda_0))$. On the other hand, ERROR2 is $O(\epsilon^2)$, because errors are divided by four when ϵ is divided by two. This is due to the fact that the term $\epsilon\alpha_0 J\nabla I(z(s_0, \lambda_0))$ has been incorporated to the perturbed equilibrium and that the initial perturbation does not have a component in the direction of M ($v_M = 0$); therefore $\rho(t) = 0$. Finally, the bounded behaviour of ERROR1 for this perturbation is also observed, while ERROR2 incorporates the time behaviour of the $O(\epsilon^2)$ terms, which seems to be linear.

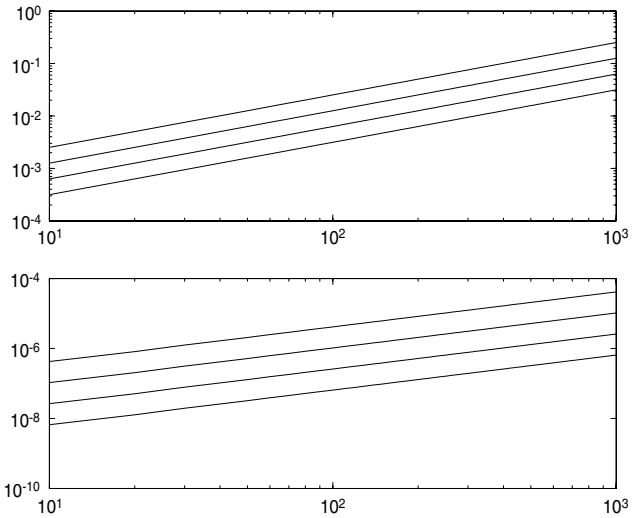

Fig. 2. Numerical illustration of (16), with $v_0 = \partial z(s_0, \lambda)/\partial\lambda|_{\lambda=\lambda_0}$ and $\epsilon = 1.25\text{E}{-}04, 6.25\text{E}{-}05, 3.125\text{E}{-}05, 1.5625\text{E}{-}05$. Top: ERROR1 against time. Bottom: ERROR2 against time. The scale is logarithmic.

Second perturbation

Here we have taken $v_0 = \partial z(s_0, \lambda)/\partial\lambda|_{\lambda=\lambda_0}$. We observe some differences with respect to the previous experiment. Now the perturbation has only one component in the direction of $\operatorname{Ker} L^2 \setminus \operatorname{Ker} L$. In this case $\alpha_0 = 0$, $\beta_0 = 1$ and $v_M = 0$ in (16). This implies again that $\rho(t) = 0$. The results are displayed in Fig. 2.

Again, since we do not have a component in M, the error with respect to the perturbed relative equilibrium is $O(\epsilon^2)$, as it is observed in the corresponding bottom figure. On the other hand, ERROR1 is $O(\epsilon)$. In this case, this is due to the first order term

$$\epsilon \left(\left. \frac{\partial z(s_0, \lambda)}{\partial \lambda} \right|_{\lambda=\lambda_0} + tJ\nabla I\,(z(s_0, \lambda_0)) \right). \tag{29}$$

This term is also visible in the linear in time behaviour of ERROR1, which has to be compared with the bounded behaviour observed in the previous experiment. With this second perturbation, the errors with respect to the unperturbed relative equilibrium are bigger than those of the first perturbation.

Third perturbation

In this example, we have considered $v_0 = (0, 0, 0, 0, 1, 0, 0, 0)$. The most important difference with the other examples is that now v_0 contains a component in the direction of the subspace M. Explicitly, we have

$$\alpha_0 = 0, \qquad \beta_0 = -\frac{3\lambda_0}{2}, \qquad v_M = \left(0, \frac{\lambda_0}{2}, 0, -\frac{\lambda_0}{2}, 0, 0, 1, 0\right).$$

The results are presented in Fig. 3.

In this case, errors with respect to the perturbed relative equilibrium are $O(\epsilon)$. This is due to the complementary term $\epsilon\rho(t)$ of (16), that is in the direction of M. On the other hand, the behaviour of ERROR1 is similar to that of the previous experiment; the leading term of the error, out of $\epsilon\rho(t)$, is of the same type as (29). The linear growth with time can be observed as well. On the other hand, the time evolution of ERROR2 illustrates the bounded in time behaviour of the complementary term. This is justified by the fact that the symmetry group consists of rotations and that the original relative equilibrium is stable.

4.3. Illustration of the structure of the numerical solution

Now we focus on formula (25). Our objective is to analyze time behaviour of numerical methods when integrating perturbations of relative equilibria.

There are several aspects to illustrate in (25). We are interested in the behaviour of the $O(h^r)$ terms. There are terms that grow with time (linearly or quadratically, depending on the conservative character of the method) and bounded terms. We will perform experiments in order to see both states.

As far as the growing terms are concerned, they can be computed in two ways. First, we can compare with the 'exact' solution. But it is also interesting (specially for some kind of perturbations) to compare with the perturbed relative equilibrium presented in (16). We will illustrate both alternatives.

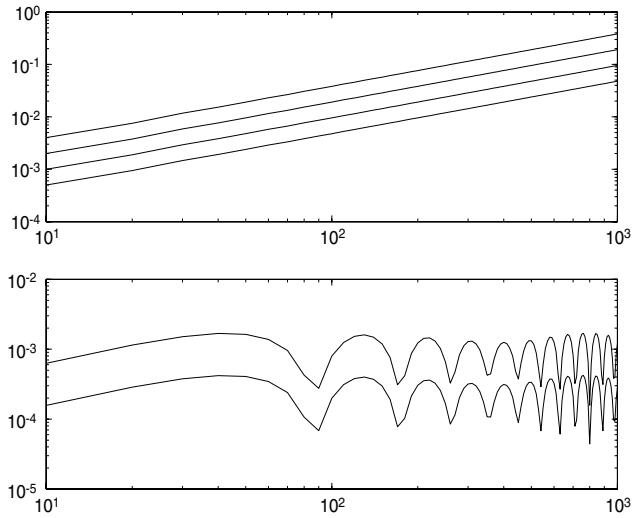

Fig. 3. Numerical illustration of (16), with $v_0 = (0, 0, 0, 0, 1, 0, 0, 0)$. Top: ERROR1 against time with $\epsilon = 1.25\text{E}{-}04, 6.25\text{E}{-}05, 3.125\text{E}{-}05, 1.5625\text{E}{-}05$. Bottom: ERROR2 against time with $\epsilon = 1.25\text{E}{-}04, 3.125\text{E}{-}05$. The scale is logarithmic.

On the other hand, in order to observe the bounded terms, we will also compare the numerical integrators with the modified perturbed relative equilibrium, which is the first term of (25). With an appropriate relation between ϵ and h, we can see the bounded behaviour of the two complementary terms in (25).

At this point, we introduce the following numerical integrators:

- The one-stage Gauss method of order two; that is, the Implicit Midpoint Rule (IMR). This method preserves the invariant I of our test problem, but not the Hamiltonian.
- The Simply Diagonally Implicit Runge Kutta method (SDIRK3),

$$\begin{array}{c|cc} \gamma & \gamma & 0 \\ 1-2\gamma & 1-2\gamma & \gamma \\ \hline & 1/2 & 1/2 \end{array}$$

  with $\gamma = (3+\sqrt{3})/6$. This method has order three and does not conserve any of the invariants of the test problem. It has been chosen to illustrate the behaviour of a typical nonconservative scheme.

Note that we could have chosen a Hamiltonian preserving method instead of the IMR. The behaviour of a conservative scheme is determined by the fact that $\beta = 0$ in formula (25). This is directly satisfied by an I-preserving method (as the IMR or, for instance, any explicit symplectic method [41]). But if a method conserves the Hamiltonian, the relation (3) between the gradients of both quantities I and H at the relative equilibria forces the condition $\beta = 0$ to be also satisfied. Therefore, in these experiments, the behaviour of an I-preserving method and a Hamiltonian preserving method is similar.

Error growth in a general perturbation

We start by considering a typical general perturbation $v_0 = (0, 0, 0, 0, 1, 0, 0, 0)$, in the sense that this has components in the two directions. The parameters are $\delta = 0.1$, $\epsilon = 1\text{E}{-}04$.

As far as the time propagation of the error is concerned, in Fig. 4 we show, in logarithmic scale, the evolution of the error, for some values of h, up to the final time $t = 1000$. Solid lines correspond to IMR and dashed lines to SDIRK3. The slopes show that, for IMR, errors grow linearly with time, while for SDIRK3, the growth is quadratic. The distance between the errors with two consecutive values of h shows the order of the methods. This behaviour is similar to the one obtained by integrating an exact relative equilibrium. In the case of IMR, formula (25) says that the method gives linear in time terms. On the other hand, SDIRK3 has a leading term of the local error that does not satisfy the condition $\beta = 0$. This implies that the scheme provides time quadratic terms in the asymptotic expansion. Recall that we are comparing with an 'exact' solution. Consequently, the $O(\epsilon)$ terms are included in it.

Error growth in a perturbation in the direction of $\mathrm{Ker}_g L$

Another way to illustrate formula (25) is to compare the corresponding numerical approximation with the perturbed relative equilibrium. In order to see the differences in the behaviour of conservative and nonconservative schemes, we shall take care with the relation between ϵ and h^r. Furthermore, we shall take a perturbation with only a component in the direction of $\mathrm{Ker}_g L$. Then, $\rho(t) = 0$ in (25).

Under these conditions, we have considered $v_0 = \partial z(s_0, \lambda)/\partial\lambda|_{\lambda=\lambda_0}$ and $\delta = 0.1$, $\epsilon = 1\text{E}{-}04$. Fig. 5 describes something similar to that of Fig. 4. The difference is that we have measured, for both methods, the evolution of the error between the

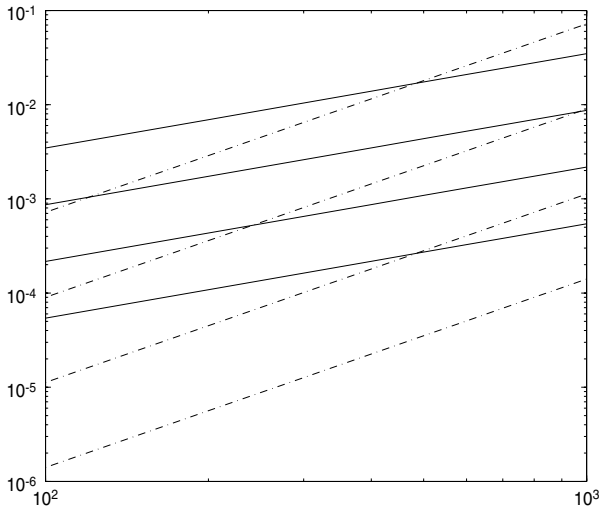

Fig. 4. Error vs. time. Solid lines: IMR, dashed lines: SDIRK3. $\epsilon = 1E{-}04$, $h = 5E{-}03$, $2.5E{-}03$, $1.25E{-}03$, $0.625E{-}03$.

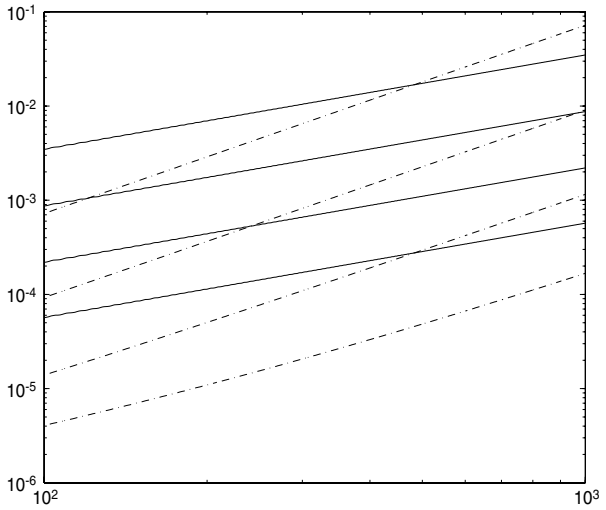

Fig. 5. Error with respect to the perturbed relative equilibrium vs time. Solid lines: IMR, dashed lines: SDIRK3. $\epsilon = 1E{-}04$, $h = 5E{-}03$, $2.5E{-}03$, $1.25E{-}03$, $0.625E{-}03$.

corresponding numerical solution and the perturbed relative equilibrium. Again, we have a linear error growth for IMR (solid lines) and quadratic error growth for SDIRK3 (dashed lines), while the order of each method is also observed (with these parameters for the problem, the $O(h^r)$ terms in formula (25) are dominant). This confirms the theoretical results.

Bounded terms

A final question we study about formula (25) is the behaviour of the complementary terms. To see this, we have considered the perturbation $v_0 = (0, 0, 0, 0, 1, 0, 0, 0)$, with components in the two directions. Recall that, since the relative equilibrium is stable, the two complementary terms are bounded in time.

Two remarks are necessary. First, note that we now compare with the modified perturbed relative equilibrium, that is, the first term on the right hand side of (25). Then we have to compute the constants α, β for the method used. Secondly, we must select different values of ϵ and h, depending on if we want to see the $O(\epsilon)$ or the $O(h^r)$ bounded term.

For this third experiment we have taken the conservative scheme IMR. In this case, $\beta = 0$ in (24). We have computed α in (23) by using extrapolation, to estimate the leading term of the local error at the relative equilibrium, in a standard way [37,42].

Fig. 6 shows the evolution of the error between the numerical solution of IMR and the modified perturbed relative equilibrium. The parameters are $\epsilon = 1E{-}03$, $h = 1.56E{-}04$ with a final time of $t = 1000$. Note that the result has a bounded behaviour. The sizes of ϵ and h considered implies that in this case the dominant term is $O(\epsilon)$, provided by the perturbation. Similarly, Fig. 7 displays the evolution of this error with $\epsilon = 1E{-}06$, $h = 1E{-}01$. in this case, the figure

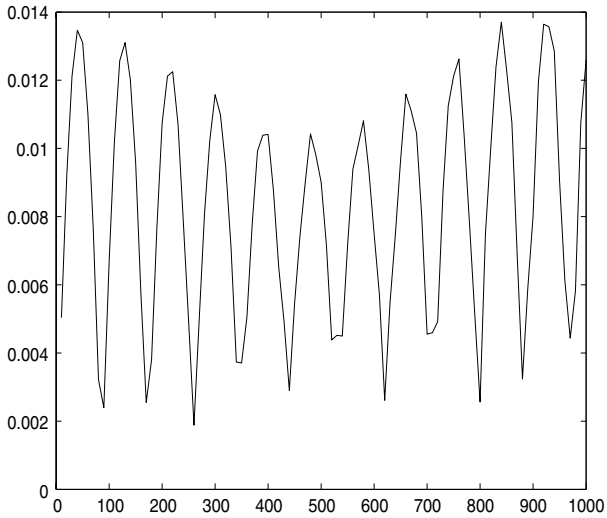

Fig. 6. Error with respect to the modified perturbed relative equilibrium vs. time. IMR with $\epsilon = 1\text{E}{-}03$, $h = 1.56\text{E}{-}04$.

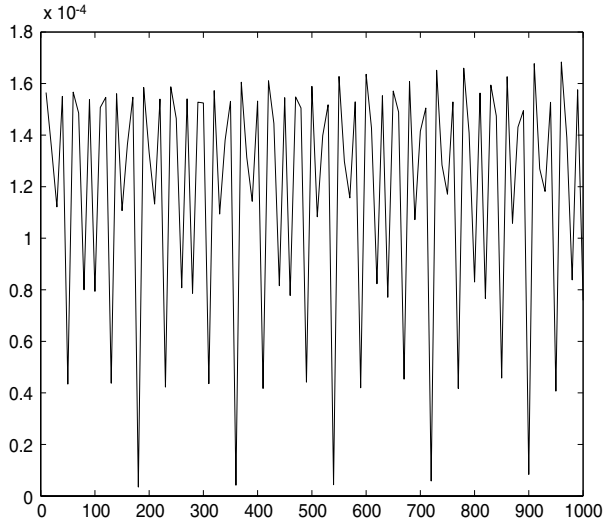

Fig. 7. Error with respect to the modified perturbed relative equilibrium vs. time. IMR with $\epsilon = 1\text{E}{-}06$, $h = 1\text{E}{-}01$.

shows the bounded behaviour of the second complementary term $O(h^r)$, provided by the numerical method. However, in both cases it is expected that, for longer times, this bounded behaviour will be dominated by the growth of the remainder terms, of order $O(\epsilon^2)$ or $O(h^{r+1})$.

Acknowledgements

This work was supported by: Ministerio de Ciencia e Innovación, under projects MTM2008-00700/MTM, MTM2008-01396-E and MTM2009-06507-E; Junta de Castilla y León, under projects VA001A08 and VA060A09 and Consolider Ingenio Mathematica, under project SAIRT-C4-0189.

References

[1] E. Hairer, Ch. Lubich, G. Wanner, Geometric Numerical Integration. Structure-Preserving Algorithms for Ordinary Differential Equations, in: Springer Series in Comput. Mathematics, vol. 31, Springer, Berlin, 2002.
[2] J.M. Sanz-Serna, Geometric integration, in: I.S. Duff, G.A. Watson (Eds.), The State of the Art in Numerical Analysis, Clarendon, Oxford, 1997, pp. 121–143.
[3] J.M. Sanz-Serna, M.P. Calvo, Numerical Hamiltonian Problems, Chapman and Hall, London, 1994.
[4] B. Leimkuhler, S. Reich, Simulating Hamiltonian Dynamics, Cambridge University Press, Cambridge, 2004.
[5] C.J. Budd, M.D. Piggott, Geometric integration and its applications, unpublished notes.

[6] E. Hairer, Ch. Lubich, The life-span of backward error analysis for numerical integrators, Numer. Math. 76 (1997) 441–462.
[7] E. Hairer, Ch. Lubich, Symmetric multistep methods over long times, Numer. Math. 97 (2004) 699–723.
[8] D.J. Estep, A.M. Stuart, The rate of error growth in Hamiltonian-conserving integrators, Z. Angew. Math. Phys. 46 (1995) 407–418.
[9] C.W. Gear, Invariants and numerical methods for ODEs, Physica D 60 (1992) 303–310.
[10] B. Cano, J.M. Sanz-Serna, Error growth in the numerical integration of periodic orbits, with application to Hamiltonian and reversible systems, SIAM J. Numer. Anal. 34 (1997) 1391–1417.
[11] B. Cano, J.M. Sanz-Serna, Error growth in the numerical integration of periodic orbits by multistep methods, with application to reversible systems, IMA J. Numer. Anal. 18 (1998) 57–75.
[12] B. Cano, A. Durán, Analysis of variable-stepsize linear multistep methods with special emphasis on symmetric ones, Math. Comp. 72 (2003) 1769–1801.
[13] B. Cano, A. Durán, An effective technique to construct symmetric variable-stepsize linear multistep methods for second-order systems, Math. Comp. 72 (2003) 1803–1816.
[14] S. Reich, Backward error analysis for numerical integrators, SIAM J. Numer. Anal. 36 (1999) 1549–1570.
[15] E. Hairer, Ch. Lubich, Long-time energy conservation of numerical methods for oscillatory differential equations, SIAM J. Numer. Anal. 38 (2001) 414–441.
[16] E. Hairer, Ch. Lubich, Oscillations over long times in numerical Hamiltonian systems, in: B. Engquist, A. Fokas, E. Hairer, A. Iserles (Eds.), Highly Oscillatory Problems, in: LMS, Lecture Notes Series, vol. 366, Cambridge University Press, 2009.
[17] A. Arakawa, Computational design for long-term numerical integration of equations of fluid motion: two-dimensional incompressible flow. Part I, J. Comput. Phys. 1 (1966) 119–143.
[18] T.J. Bridges, Multi-symplectic structures and wave propagation, Math. Proc. Cambridge Philos. Soc. 121 (1997) 147–190.
[19] T.J. Bridges, S. Reich, Multi-symplectic integrators: numerical schemes for Hamiltonian PDEs that conserve symplecticity, Phys. Lett. A 284 (2001) 184–193.
[20] S. Reich, Multi-symplectic Runge–Kutta collocation methods for Hamiltonian wave equations, J. Comput. Phys. 157 (2000) 473–499.
[21] D. Cohen, E. Hairer, Ch. Lubich, Long-time analysis of nonlinearly perturbed wave equations via modulated Fourier expansions, Arch. Ration. Mech. Anal. 187 (2008) 341–368.
[22] J. de Frutos, J.M. Sanz-Serna, Accuracy and conservation properties in numerical integration: the case of the Korteweg–de Vries equation, Numer. Math. 75 (1997) 421–445.
[23] A. Durán, J.M. Sanz-Serna, The numerical integration of relative equilibrium solutions. The nonlinear Schrödinger equation, IMA J. Numer. Anal. 20 (2000) 235–261.
[24] A.L. Islas, D.A. Karpeev, C.M. Schober, Geometric integrators for the nonlinear Schrödinger equation, J. Comput. Phys. 173 (2001) 116–148.
[25] B. Cano, Conserved quantities of some Hamiltonian wave equations after full discretization, Numer. Math. 103 (2006) 197–223.
[26] M. Oliver, M. West, C. Wulff, Approximate momentum conservation for spatial semidiscretizations of nonlinear wave equations, Numer. Math. 97 (2004) 493–535.
[27] P.J. Olver, Applications of Lie Groups to Differential Equations, Springer, New York, 1986.
[28] J.E. Marsden, Lectures on Mechanics, Cambridge University Press, Cambridge, 1992.
[29] J.E. Marsden, T.S. Ratiu, Introduction to Mechanics and Symmetry, Springer, New York, 1994.
[30] V.I. Arnold, Mathematical Methods of Classical Mechanics, Springer, Berlin, 1989.
[31] P.G. Drazin, R.S. Johnson, Solitons: An Introduction, Cambridge University Press, Cambridge, 1989.
[32] C. Wulff, M. Roberts, Hamiltonian systems near relative periodic orbits, SIAM J. Appl. Dyn. Syst. 1 (2002) 1–43.
[33] B. Cano, A. Durán, A technique to improve the error propagation when integrating relative equilibria, BIT 44 (2004) 215–235.
[34] A. Durán, J.M. Sanz-Serna, The numerical integration of relative equilibrium solutions. Geometric theory, Nonlinearity 11 (1998) 1547–1567.
[35] T.J. Bridges, Degenerate relative equilibria, curvature of the momentum map and homoclinic bifurcation, J. Differential Equations 244 (2008) 1629–1674.
[36] R.L. Pego, M.I. Weinstein, Asymptotic stability of solitary waves, Comm. Math. Phys. 164 (1994) 305–349.
[37] E. Hairer, S.P. Nørsett, W.G. Wanner, Solving Ordinary Differential Equations I, Nonstiff Problems, 2nd ed., Springer, Berlin, 1993.
[38] P. Henrici, Discrete Variable Methods in Ordinary Differential Equations, John Wiley & Sons, New York, 1961.
[39] A. Durán, M.A. López-Marcos, Numerical behaviour of stable and unstable solitary waves, Appl. Numer. Math. 42 (2002) 95–116.
[40] L. Dieci, R.D. Russell, E.S. van Vleck, Unitary integrators and applications to continuous orthonormalization techniques, SIAM J. Numer. Anal. 31 (1994) 261–281.
[41] E. Hairer, Ch. Lubich, G. Wanner, Geometric numerical integration illustrated by the Störmer–Verlet method, Acta Numer. 12 (2003) 399–450.
[42] L.F. Richardson, The approximate arithmetical solution by finite differences of physical problems including differential equations, with application to the stresses in a masonry dam, Philos. Trans. R. Soc. Lond. Ser. A 210 (1910) 307–357.